

**ORIGINAL ARTICLE**

# Geometric accuracy of magnetic resonance imaging-derived virtual 3-dimensional bone surface models of the mandible in comparison to computed tomography and cone beam computed tomography: A porcine cadaver study

Florian Andreas Probst MD, DMD, PhD<sup>1</sup>  | Egon Burian MD, DMD<sup>2</sup> |  
Yoana Malenova DMD<sup>1</sup> | Plamena Lyutskanova DMD<sup>1</sup> |  
Maria Juliane Stumbaum DMD<sup>3</sup> | Lucas Maximilian Ritschl MD, DMD, PhD<sup>4</sup> |  
Sophia Kronthaler M.Sc.<sup>5</sup> | Dimitrios Karampinos PhD<sup>5</sup> | Monika Probst MD<sup>2</sup>

<sup>1</sup>Department of Oral and Maxillofacial Surgery and Facial Plastic Surgery, University Hospital, LMU München, Munich, Germany

<sup>2</sup>Department of Diagnostic and Interventional Neuroradiology, Klinikum Rechts der Isar, School of Medicine, Technical University of Munich, Munich, Germany

<sup>3</sup>Department of Prosthetic Dentistry, University Hospital, LMU München, Munich, Germany

<sup>4</sup>Department of Oral and Maxillofacial Surgery, Klinikum Rechts der Isar, School of Medicine, Technical University of Munich, Munich, Germany

<sup>5</sup>Department of Diagnostic and Interventional Radiology, Klinikum Rechts der Isar, School of Medicine, Technical University of Munich, Munich, Germany

**Correspondence**

Florian Andreas Probst, MD, DMD, PhD,  
Department of Oral and Maxillofacial Surgery and Facial Plastic Surgery, University Hospital, LMU München, Lindwurmstr. 2a, 80337 Munich, Germany.  
Email: florian.probst@med.uni-muenchen.de

**Abstract**

**Background:** Providing accurate 3-dimensional virtual bone surface models is a prerequisite for virtual surgical planning and additive manufacturing in craniomaxillofacial surgery. For this purpose, magnetic resonance imaging (MRI) may be a radiation-free alternative to computed tomography (CT) and cone beam computed tomography (CBCT).

**Purpose:** The aim of this study was to assess the geometric accuracy of 3-dimensional T1-weighted MRI-derived virtual bone surface models of the mandible in comparison to CT and CBCT.

**Materials and methods:** Specimens of the mandible from porcine cadavers were scanned with (1) a 3-dimensional T1-weighted MRI sequence (0.6 mm isotropic voxel) optimized for bone imaging, (2) CT, and (3) CBCT. Cortical mandibular structures ( $n = 10$ ) were segmented using semiautomated and manual techniques. Imaging-based virtual 3-dimensional models were aligned with a high-resolution optical 3-dimensional surface scan of the dissected bone (=ground truth) and global geometric deviations were calculated (mean surface distance [MSD]/root-mean-square distance [RMSD]). Agreement between the imaging modalities was assessed by equivalence testing and Bland–Altman analysis.

**Results:** Intra- and inter-rater agreement was on a high level for all modalities. Global geometric deviations (MSD/RMSD) between optical scans and imaging modalities were  $0.225 \pm 0.020$  mm/ $0.345 \pm 0.074$  mm for CT,  $0.280 \pm 0.067$  mm/ $0.371 \pm 0.074$  mm for MRI, and  $0.352 \pm 0.076$  mm/ $0.454 \pm 0.071$  mm for CBCT. All imaging modalities were statistically equivalent within an equivalence margin of  $\pm 0.3$  mm, and Bland–Altman analysis indicated high agreement as well.

This is an open access article under the terms of the Creative Commons Attribution-NonCommercial-NoDerivs License, which permits use and distribution in any medium, provided the original work is properly cited, the use is non-commercial and no modifications or adaptations are made.

© 2021 The Authors. *Clinical Implant Dentistry and Related Research* Published by Wiley Periodicals LLC

**Conclusions:** The results of this study indicate that the accuracy and reliability of MRI-derived virtual 3-dimensional bone surface models is equal to CT and CBCT. MRI may be considered as a reliable alternative to CT and CBCT in computer-assisted craniomaxillofacial surgery.

#### KEYWORDS

additive manufacturing, CAD/CAM, computer-assisted surgery, craniomaxillofacial surgery, dental imaging, guided-implant surgery, image processing, implant surgery, magnetic resonance imaging, radiology

#### What is known

- MRI is suitable for imaging of cortical and cancellous bone on the basis of dedicated sequences.
- Little is known on accuracy of virtual MRI-derived bone surface models.
- Accurate virtual bone models are a prerequisite for computer-assisted surgery.

#### What this study adds

- The study provides data on the geometric accuracy of MRI-derived virtual 3-dimensional bone surface models of the mandible in comparison to CT and CBCT.

## 1 | INTRODUCTION

Computer-assisted surgical procedures have gained considerable importance in dentistry and craniomaxillofacial surgery in recent years, and it seems likely that this trend will accelerate further. Important application areas include orthognathic surgery,<sup>1</sup> dental implantology,<sup>2,3</sup> maxillofacial trauma,<sup>4</sup> craniomaxillofacial reconstruction,<sup>5</sup> and craniofacial malformation.<sup>6</sup> The process of the computer-aided surgery (CAS) follows a characteristic sequence. Starting with data acquisition provides a digital images and communications in medicine (DICOM) file. The following step comprises image processing with segmentation and conversion of images to 3-dimensional surface models followed by virtual surgical planning (VSP) using a dedicated software. Finally, the planning is transferred into the operation via additive manufactured accessories like drilling guides, templates, patient-specific implants, or intraoperative navigation commonly based on standard tessellation language (STL) files. A common summarization of these processes is also given by the term computer-aided design/computer-aided manufacturing (CAD/CAM) procedures. Currently, computed tomography (CT) or cone beam computed tomography (CBCT) are routinely used as the imaging modality of choice for VSP due to their ability to appropriately visualize bone structures. However, both imaging modalities have the major disadvantage because they expose patients to ionizing radiation. Despite constant efforts to further reduce the radiation dose,<sup>7,8</sup> CT and CBCT remain invasive, and studies suggest that diagnostic radiation exposure from dental X-rays might be associated with an increased risk of thyroid cancer and meningioma.<sup>9,10</sup> Finally, the radiation applied when using CT or CBCT is a major drawback and a principle factor limiting the further progression of VSP in dentistry and craniomaxillofacial surgery. This is particularly true for elective

procedures like implant surgery and orthognathic surgery, for applications that may benefit from multiple follow-up imaging and for use on young patients. Magnetic resonance imaging (MRI) is a principle 3-dimensional cross-sectional imaging alternative to CT and CBCT, which does not depend on the use of ionizing radiation. For a long time, the focus of MRI was mainly on soft tissue imaging. However, it has become increasingly apparent in recent years that MRI can also be used in musculoskeletal imaging including the quantification of cortical and cancellous bone based on sequences such as ultra-short echo time (UTE).<sup>11-13</sup>

Recently, MRI is also increasingly becoming the focus of attention in dentistry and craniomaxillofacial surgery because 3 Tesla (3T) MRI scanners using 3-dimensional high-resolution isotropic resolution sequences and dedicated radiofrequency (RF) coils currently enable dental imaging with a significant increase in resolution, improvement of the signal-to-noise ratio, reduction in acquisition times, and artifact suppression.<sup>14-18</sup> High agreement concerning linear measurements of the mandible between MRI and CT has been reported.<sup>15,19-21</sup> Moreover, MRI-derived virtual 3-dimensional models of the mandibular bone and their conversion to STL files have been described. This can be seen as a prerequisite for linking MR imaging to a digital workflow in CAS.<sup>22</sup> A few further cadaver studies reported on the accuracy of MRI-derived 3-dimensional models in comparison to CT for the lower extremities<sup>23-27</sup> but there are no data comparing MRI-derived surface models to those derived from CBCT.

Regardless of the fact that MR imaging protects patients from radiation exposure, it has diagnostic added value compared to CT and CBCT due to its excellent soft tissue depiction. Accordingly, relevant parts of the dental and facial anatomy such as dental pulp and mucosa or neurovascular structures, skin, and subcutaneous tissues may be better integrated into the virtual planning process.<sup>28-33</sup>

There is still little evidence that MRI is able to depict maxillofacial cortical bone structures quantitatively on the same level as CT or CBCT imaging, thus substantiating that MRI can serve as a reliable imaging modality for VSP and additive manufacturing in dentistry and craniomaxillofacial surgery. Therefore, the aim of this study was to assess the geometric accuracy of 3-dimensional T1-weighted MRI-derived virtual 3-dimensional bone surface models of the mandibular body in comparison to CT and CBCT.

## 2 | MATERIAL AND METHODS

### 2.1 | Study design

The prospective study was planned and performed according to the STARD guidelines. The Municipal Veterinary Office (city of Munich, Germany) approved the cadaveric study. Porcine cadaver mandibles (domestic pigs, mixed dentition) with surrounding soft tissue were used as samples. The region of interest (ROI) and subject of the study was one side of the mandibular body ( $n = 10$ ). The maximum dimensions of the samples did not exceed  $100 \times 50 \times 30$  mm (anteroposterior  $\times$  cranial-caudal  $\times$  horizontal). The study design is illustrated in Figure 1.

### 2.2 | Magnetic resonance imaging

All specimens underwent MRI on a 3T system (Elition, Philips Healthcare, Best, the Netherlands). The specimens were placed in a plastic box filled with water, the occlusal plane was roughly oriented parallel to the scanner table, and a 16-channel Head and Neck Spine

array was placed around the box. A 3-dimensional T1-weighted MR sequence with an isotropic-resolution of 0.6 mm was chosen, which is optimized for bone visualization and already in clinical use.<sup>32</sup> To reduce the echo time partial Fourier imaging was employed in the frequency encoding direction with a factor of 60%.<sup>34</sup> The specifications for the 3-dimensional T1-weighted bone sequence are displayed in Table 1.

### 2.3 | CT and CBCT scanning

Multislice CT scans were performed using a Philips Ingenuity 128 device (Philips Healthcare, Best, the Netherlands). Specimens were positioned on the CT table with the occlusal plane aligned parallel

**TABLE 1** Specifications of MRI – 3-dimensional T1-weighted bone sequence

MRI – 3-dimensional T1-weighted bone sequence	
Acquisition time	03:08 min
FOV	180 mm
Matrix	420 $\times$ 419
Acquired voxel	0.6 $\times$ 0.6 $\times$ 0.6 mm <sup>3</sup>
Number of signal averages	1
TR	10 ms
TE	1.53 ms
CS + SENSE	yes
Reduction	2.3

Abbreviations: CS, compressed sensing; FOV, field of view; SENSE, sensitivity encoding; TE, echo time; TR, repetition time.

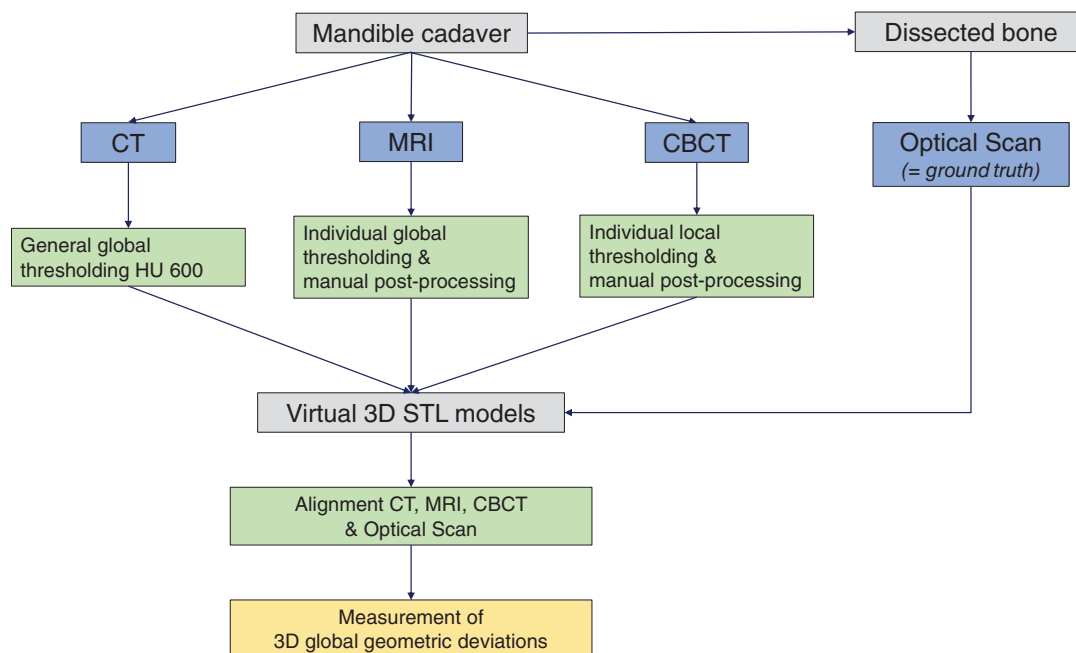


**FIGURE 1** Outline of the study

to the floor. Isotropic voxel size was 0.67 mm, field of view (FOV) 20 × 20 cm, tube voltage 120 kV, and tube current time product was 250 mAs. Cone beam computed tomography was carried out using a Carestream CS 9300 device (Carestream Dental LLC, Atlanta, GA). Specimens were positioned on a plate mounted on a photo tripod to imitate the positioning of a patient with the occlusal plane oriented nearly parallel to the floor. Isotropic voxel size was 0.18 mm, field of view 10 × 10 cm, tube voltage 90 kV, and tube current time product was 25.6 mAs.

## 2.4 | Optical scan of cadaver bone surface

All soft tissues of the cadaveric specimens were removed from cortical bone after CT, MRI, and CBCT imaging, in order to create an optical 3-dimensional surface scan of the bone, serving as ground truth.<sup>35</sup> Therefore, the specimens were mechanically cleaned with standard dissection equipment like scalpels and scrapers. No boiling or chemical treatments were used because it is known that these treatments can introduce geometric deviations due to shrinking effects on the bone interface.<sup>27,36</sup> Subsequently, a high-resolution optical 3-dimensional scanner (Artec Space Spider, Artec 3D, Luxembourg) with a stated resolution up to 0.1 mm and a point accuracy up to 0.05 mm was used to capture 3-dimensional images of the cadaveric bone surface. The data were further processed by the corresponding software (Artec Studio 14, Artec 3D, Luxembourg) using the autopilot tool, resulting in a final rendered 3-dimensional surface scan. That was exported as an STL file and served as reference (=ground truth).

## 2.5 | Image processing and segmentation procedures

DICOM data of MRI, CT, and CBCT were imported into specialized medical image processing software (Mimics, Materialise; Leuven, Belgium). Cortical bone of the mandibular body was segmented in MRI, CT, and CBCT images (Figure 2).

With respect to CT data, cortical bone was automatically segmented by applying a general global threshold of the Hounsfield scale to all samples. For this purpose, all voxels with Hounsfield units (HU) of 600 and above were selected in each specimen. This threshold was set after a review of CT images and HU histograms and in agreement with two radiologists and one oral and maxillofacial surgeon.

Regarding the MRI segmentation, specimen-individual global thresholds of the signal intensity range were defined for each sample in agreement with two radiologists and one oral and maxillofacial surgeon. Subsequently, the cortical bone boundaries had to be manually postprocessed using a range of tools of the imaging software.

For the CBCT segmentation, specimen-individual local thresholds were first applied to different regions of the mandibular body. In this method, also known as multilevel thresholding, an image is divided into several ROIs, for which an individual threshold bandwidth is selected.<sup>35</sup> In a second step, the borders of the cortical bone were selected manually with different tools of the image processing software.

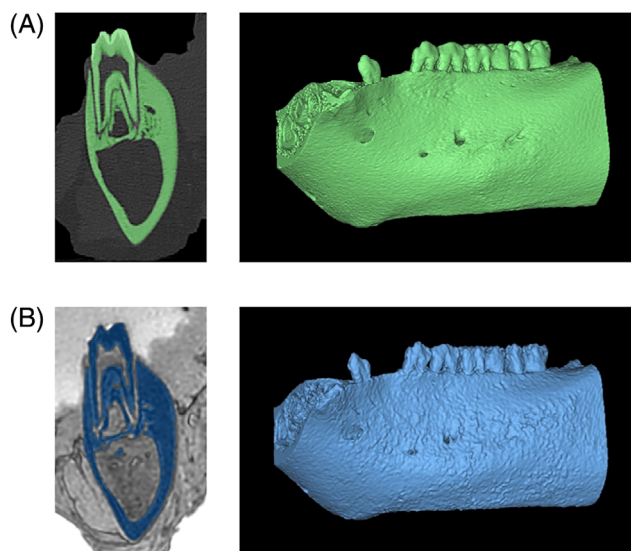


**FIGURE 2** Segmentation (left) and conversion to 3-dimensional models (right) of (A) CT and (B) MRI images

Based on the segmented parts, 3-dimensional objects of the cortical bone and teeth were generated and converted to STL models (Figure 2). CT-, CBCT-, and MRI-derived 3-dimensional STL models as well as the STL files of the corresponding optical scans (=ground truth) were imported into 3-dimensional modeling software (3-matic, Materialise; Leuven, Belgium). Three-dimensional models of CT, CBCT, and MRI were aligned with the 3-dimensional model of the corresponding high-resolution optical scan first by a three-point alignment procedure followed by global alignment (10 iterations, stepwise reduction of agreement down to a level of approximately 30 μm) (Figure 3). Based on this alignment, global 3-dimensional geometric deviations between the imaging modalities were measured in 3-matic (Figure 3). In this way, the shortest 3-dimensional distance (Euclidean distance) from any point on the surface of the optical scan to the target surface of the CT-, CBCT-, and MRI-derived 3-dimensional models was calculated. Mean unsigned (absolute) distances, referred to as “mean surface distance” (MSD) according to van Eijnatten and colleagues, and root-mean-square distances (RMSD) were reported.<sup>35</sup> Color-coded difference images (heatmaps) allow conclusions on the localization of areas with high or low geometric deviations. For further qualitative graphical assessment, the aligned 3-dimensional models of CT, CBCT, and MRI were transferred to Mimics while maintaining the alignment to each other. As a result, the respective contours of the 3-dimensional models can be reviewed in the multiplanar reconstructions of the different imaging modalities (Figure 4).

## 2.6 | Study variables and statistical analysis

Intra- and inter-rater agreement (two observers, repetition after 6 weeks) was determined by intraclass correlation (ICC) analyses based on root-mean-square distances (RMSD) in each group. For this

**FIGURE 3** (A) Alignment procedure of medical imaging-derived 3-dimensional surface model (yellow) with the corresponding optical scan-derived 3-dimensional model of the dissected bone (pink). (B) Global 3-dimensional geometric deviations displayed by a color map

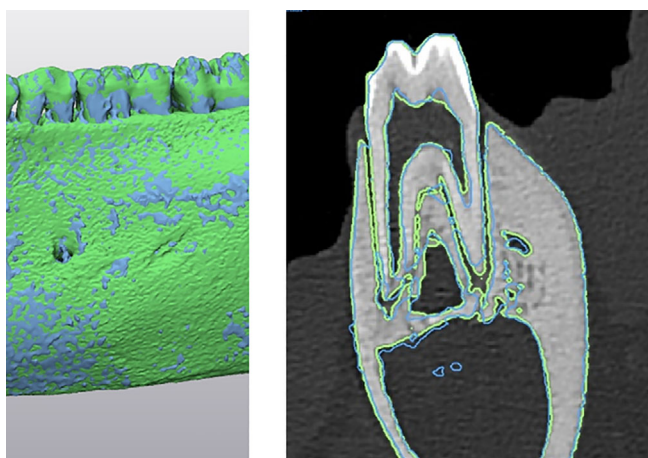
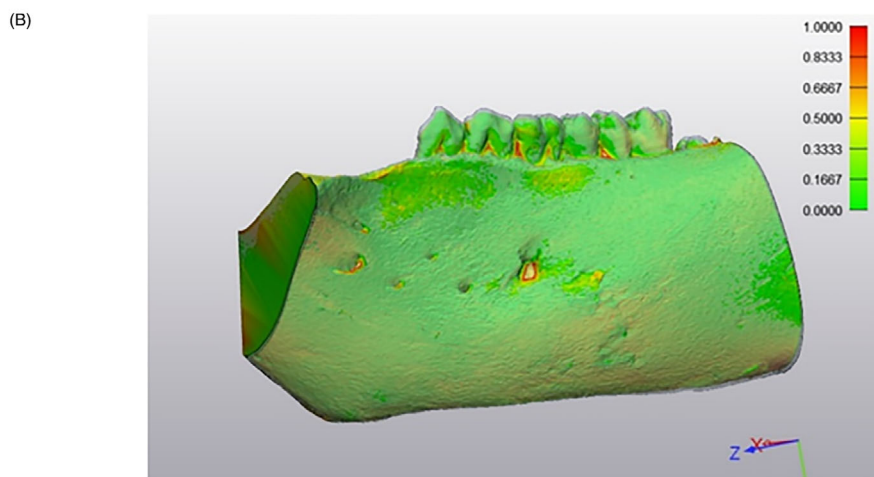
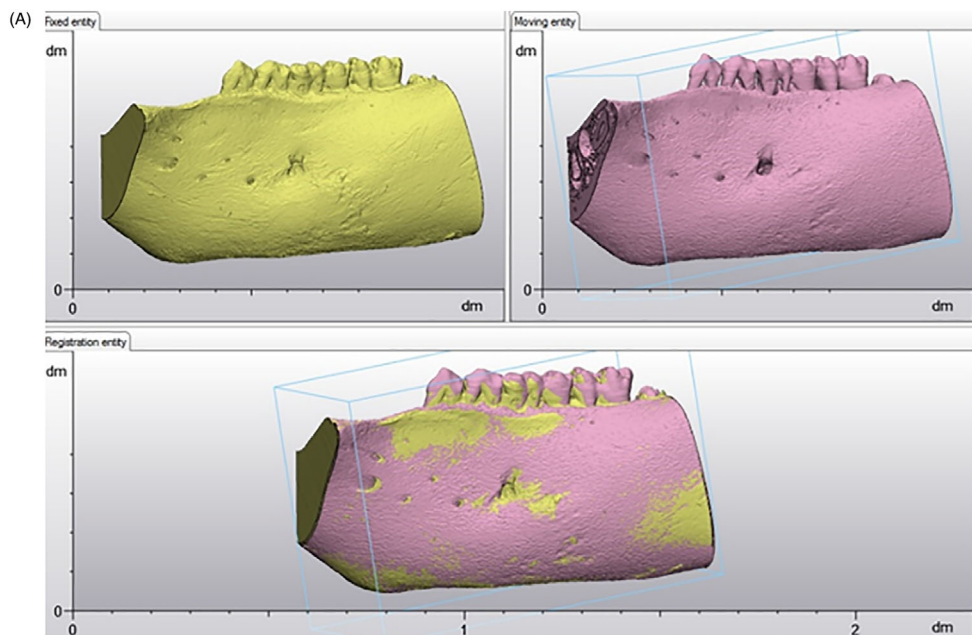


**FIGURE 4** Contours of the aligned 3-dimensional surface models (left) can be reviewed in the multiplanar reconstructions of the different imaging modalities (right). CT imaging displayed in green, MRI displayed in blue

purpose, the complete workflow including segmentation and alignment was repeated.

Global 3-dimensional geometric deviations, given as mean surface distances (MSD) and root-mean-square distances (RMSD), between the imaging modalities and the high-resolution optical scan (=ground truth) was set as the primary outcome variable.<sup>35</sup> One-way analysis of variance (ANOVA) was used to test mean differences between the groups.

Equivalence testing between the imaging modalities with two one-sided *t*-tests (TOST) was performed (RMSD values). Based on a literature review reporting on the accuracy of CT image segmentation methods for bone using global thresholding, a predefined equivalence margin ( $\pm 0.3$  mm) was set (RMSD values). This corridor can also be considered acceptable from a clinical point of view in the context of computer-assisted surgery and additive manufacturing. The level of agreement between CT, MRI, and CBCT was further assessed by Bland–Altman analysis indicating the mean differences (RMSD values)

between the imaging modalities and the upper and lower limits of agreement (LOA, mean of the differences  $\pm 1.96 \times SD$  of the differences).

Statistical analysis was carried out with Excel (Microsoft, Redmond, WA) and SPSS 25 (SPSS Inc., Chicago, IL).

### 3 | RESULTS

Between observers (inter-rater reliability), the ICC coefficients based on root-mean-square distances (RMSD) were 0.978 (CT), 0.987 (MRI), and 0.943 (CBCT). Intraobserver ICC coefficients were 0.985/0.983 (CT), 0.981/0.980 (MRI), and 0.997/0.943 (CBCT).

Averages of global 3-dimensional geometric deviations with regard to mean surface distances (MSD) between optical scans and imaging modalities were  $0.225 \pm 0.020$  mm (95% CI 0.211–0.240 mm) for CT,  $0.280 \pm 0.067$  mm (95% CI 0.232–0.328 mm) for MRI, and  $0.352 \pm 0.076$  mm (95% CI 0.298–0.407 mm) for CBCT. Only differences between CT and CBCT were statistically significant ( $p < 0.05$ , ANOVA, Games–Howell post hoc test). Averages of global 3-dimensional geometric deviations with regard to root-mean-square distances (RMSD) between optical scans and imaging modalities were  $0.345 \pm 0.074$  mm (95% CI 0.292–0.398 mm) for CT,  $0.371 \pm 0.074$  mm (95% CI 0.318–0.424 mm) for MRI, and  $0.454 \pm 0.071$  mm (95% CI 0.403–0.504 mm) for CBCT. Differences between CT and CBCT as well as between MRI and CBCT were statistically significant ( $p < 0.05$ , ANOVA, Tukey's HSD post hoc test). Results are displayed in Figure 5.

Two one-sided *t*-tests (TOST) were highly significant ( $p < 0.001$ ) between CT, MRI, and CBCT. A 90% confidence interval of the differences between the different imaging modalities remained within the predefined equivalence margin of  $\pm 0.3$  mm. Therefore, CT, MRI, and CBCT can be considered equivalent (Figure 6).

Bland–Altman analysis indicated high agreement between the different imaging modalities. There was a slight tendency for higher deviations between CT and CBCT (Figure 7).

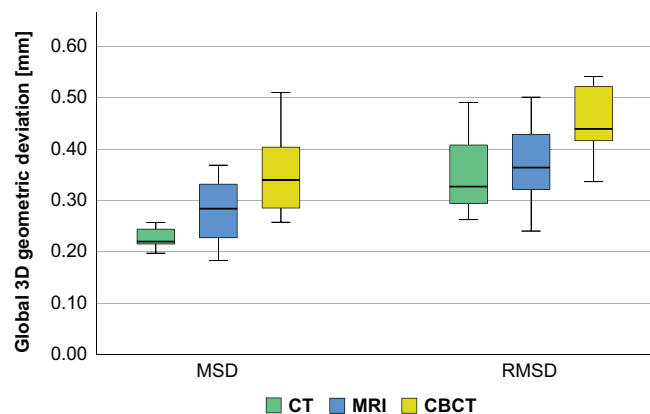


**FIGURE 5** Boxplot global 3-dimensional geometric deviations (mm) of CT, MRI, and CBCT with regard to mean surface distances (MSD, left) and root-mean-square distances (RMSD, right)

### 4 | DISCUSSION

The aim of this study was to assess the geometric accuracy of 3-dimensional T1-weighted MRI-derived virtual 3-dimensional bone surface models of the mandible in comparison to CT- and CBCT-derived bone surface models. Equivalence testing and Bland–Altman analysis indicated substantial agreement between the different imaging modalities. Notably, CBCT showed higher root-mean-square distances (RMSD) compared to CT and MRI. In summary, the results of this study indicate that the accuracy and reliability of MRI-derived virtual 3-dimensional bone surface models is equal to CT and CBCT. This has high clinical relevance because CAS is currently limited due to the radiation exposure associated with CT and CBCT as the current standard imaging modalities.

Accurate virtual 3-dimensional bone surface models of the craniomaxillofacial complex are mandatory for computer-assisted planning and additive manufacturing. Inaccuracies can occur at any step of CAS but are predominantly attributed to imaging and image processing.<sup>37–39</sup> The accuracy of the imaging procedure itself depends on the image slice thickness and slice interval. But also imaging noise, beam hardening, as well as motion and metallic artifacts, may cause inhomogeneities in CT, CBCT, and MRI images.<sup>35</sup> Imaging processing can also affect the accuracy.<sup>40</sup> The most delicate step in imaging processing is image segmentation, which means that an image is partitioned into multiple segments, for example representing different types of tissue such as bone or soft tissue.<sup>41</sup> A variety of different segmentation techniques is described, including manual segmentation, global thresholding, and advanced techniques based on statistical shape models.<sup>35</sup> According to a review on CT image segmentation provided by van Eijnatten and colleagues,<sup>35</sup> the accuracy of 3-dimensional surface models based on manual segmentation ranged

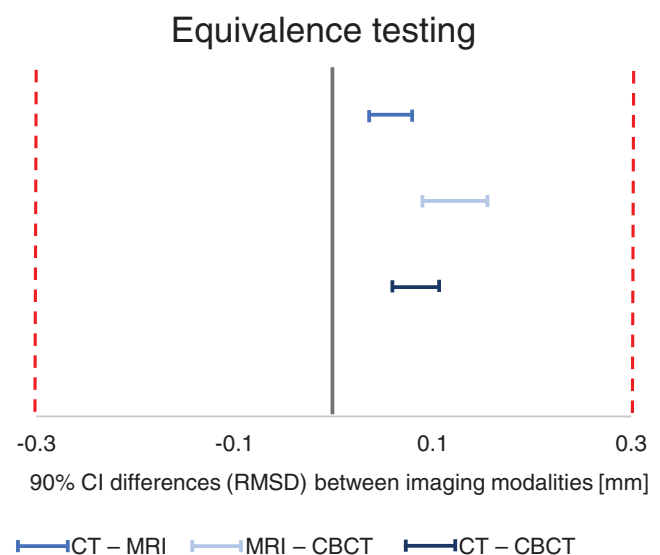


**FIGURE 6** Equivalence testing. A 90% confidence interval of the differences (root-mean-square distances, RMSD) between the different imaging modalities remained within the predefined equivalence margin of  $\pm 0.3$  mm (red vertical lines)

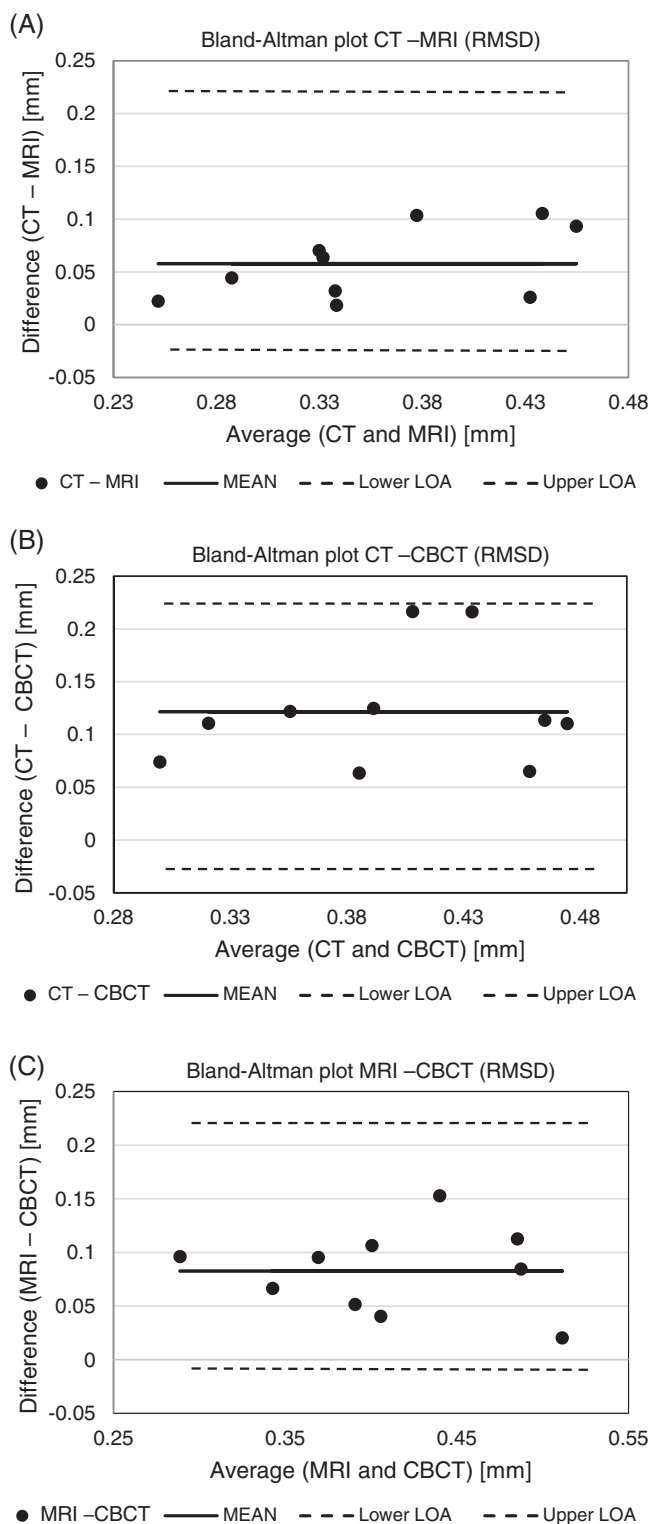


**FIGURE 7** Bland-Altman plots of the differences between (A) CT-MRI, (B) MRI-CBCT, and (C) CT-CBCT with regard to root-mean-square distances (RMSD). The solid lines represent the mean differences, the dashed lines represent the upper and lower limits of agreement (LOA)

from 0.20 to 0.48 mm. Global thresholding, the predominant segmentation technique used in clinical routine, included inaccuracies mainly between 0.1 and 0.5 mm. The geometric deviations of CT-derived

3-dimensional bone surface models in this study (MSD  $0.225 \pm 0.020$  mm, RMSD  $0.345 \pm 0.074$  mm) are in the lower middle of the corridor of previously reported accuracies, which are mainly given as mean surface distances. Based on these data and according to acceptable errors from a clinical and technical point of view, equivalence margins ( $\pm \theta$ ) of  $\pm 0.3$  mm were set for RMSD values. The differences between the geometric deviations between all three imaging modalities (CT, MRI, and CBCT) were equal within the limits of the study setting applied here. This indicates that MRI is suitable for cortical bone imaging and conversion to 3-dimensional surface models in the context of computer-assisted craniomaxillofacial surgery.

Limited previously published data are available assessing the accuracy of MRI-derived 3-dimensional bone surface models. A cadaver study based on three human mandibles compared 3-dimensional surface models based on CT and MRI with surface models based on high-resolution optical scans of the corresponding dissected bone and demonstrated larger geometric deviations in the mandibular body region in CT (range of 95th percentiles 0.3–0.62 mm) and MRI (range of 95th percentiles 0.86–1.30 mm) compared to our study.<sup>22</sup> Although comparable spatial resolution in CT and MRI was used, the differences may be explained by the fact that in contrast to this study, surface models of the whole mandible were superimposed onto each other. Three-dimensional ultrashort echo time (UTE) MRI quantitative evaluation of the temporomandibular joint condyle morphology *ex vivo* showed high correlation against micro-CT with an average geometric deviation of  $0.19 \pm 0.15$  mm.<sup>42</sup> A few more *ex vivo* studies focused on geometric deviations between CT and MRI with respect to surface models of the lower extremities. In these studies, direct comparisons of CT- and MRI-derived 3-dimensional models range from 0.19 to 0.83 mm. Comparisons to an optical scan as a ground truth range from 0.15 to 0.85 mm for CT and 0.23 to 1.3 mm for MRI.<sup>23–27</sup> However, the results between the aforementioned studies are difficult to compare because of the inhomogeneous study settings, with differing imaging devices, imaging protocols with considerably varying resolutions, regions of interest, geometric measures, and segmentation techniques as well as the presence or absence of a ground truth.

Although the differences of geometric deviations with CT and MRI were within the defined equivalence margins of this study, the accuracy of CBCT-derived surface models was significantly lower. This is remarkable because the image resolution of CBCT was clearly lower than that of CT and MRI. However, CBCT is known for lower signal-to-noise ratios, worse contrast, and higher-intensity inhomogeneity than conventional CT, making the DICOM to 3-dimensional surface model conversion more troublesome compared with CT imaging.<sup>43–46</sup> A similar experience was had in this study, with the CBCT images the most difficult to segment. When discussing the data presented here, it is important to note that the use of other segmentation protocols for the respective imaging methods might have had a significant impact on the accuracy of the derived 3-dimensional models.

The MRI protocol used in this study was previously established for optimized bone depiction in the dental and craniomaxillofacial area and is already in clinical use.<sup>32</sup> In order to decrease the echo time,

partial Fourier imaging with a factor of 60% was employed in the 3-dimensional T1-weighted bone sequence.<sup>34</sup> Further MRI techniques such as UTE imaging, zero echo time (ZTE) imaging, or sweep imaging with Fourier transformation (SWIFT) were applied to overcome the very short T2 and T2\* relaxation times in hard tissues.<sup>11,13</sup> Based on the large gradient hardware performance of the employed 3T scanner (Elition, Philips Healthcare) and due to the combination of compressed sensing (CS) with sensitivity encoding (SENSE) parallel imaging, a good signal-to-noise ratio and a short acquisition time can be achieved without the use of additional surface coils.<sup>47,48</sup>

Although this study as well as some other recent studies show that MRI is suitable for bone depiction, there is another aspect that needs to be considered in the context of CAS, in particular for the manufacturing of tooth-supported devices like drilling guides, osteotomy guides, or occlusal splints. For this purpose, the occlusal surfaces must be visible at least well enough to be able to be aligned with highly precise virtual models derived from optical surface scans.<sup>49</sup> This requirement is met with the MRI-based approach, when special devices are used at the time of MRI scanning that provide sufficient delineation of the tooth surfaces.<sup>32,50</sup>

One of the most important arguments in favor of MRI is that it involves no radiation exposure. Apart from that, there are numerous additional diagnostic benefits based on its excellent soft tissue contrast. As a result, there are a number of useful areas of application of MRI-based bone visualization and consecutive virtual 3-dimensional bone surface model generation in dentistry and craniomaxillofacial surgery. Specific clinical applications recently reported include guided dental implant surgery,<sup>32,51,52</sup> trauma surgery,<sup>30</sup> orthodontic treatment planning,<sup>21</sup> and craniostylosis surgery.<sup>53</sup> Practical limitations to the use of MR imaging in dental and craniofacial applications include the presence of motion and susceptibility artifacts, some contraindications such as the presence of pacemakers or neurostimulators, and limitations in terms of extended cost and availability.

Some limitations of the present study require further discussion. First of all, this is a cadaveric study and so the effect of movement artifacts is not considered. Although the MRI protocol allows for a relatively short acquisition time, it is significantly higher than for CT and CBCT. Besides, artifacts due to dental restorations or orthodontic appliances may affect imaging quality in MRI, although this is also true for CT and CBCT. Second, the segmentation techniques of all imaging modalities in this study are based on a manual threshold selection and thus represent to some extent a subjective process. Manual threshold selection is known to have a substantial influence on the reliability and accuracy of medical additive manufacturing.<sup>46</sup> While CT represents the gold standard for CAD/CAM procedures, the thresholding of bone-specific gray values is less straightforward in CBCT images.<sup>43-46</sup> This aspect is reflected in the present study, where the segmentation of CBCT images required individual and local thresholding followed by sometimes extensive manual post-processing. In contrast, CT imaging was performed by global thresholding without the need for manual post-processing. The segmentation procedures of MR images, including global thresholding

and only moderate manual postprocessing, were considerably more straightforward than for CBCT. Nevertheless, further progress in MRI thresholding techniques is demanded in order to optimize reliability, accuracy, and practicability, thus establishing MRI-based CAS. Automated processes will certainly play a significant role in this respect.<sup>54,55</sup> A further limitation of the study is that porcine specimens were used and that the region of interest was restricted to the mandibular body. It is known that larger regions of interest with significant geometric differences between each other, for example the whole midface complex, are more difficult to segment, and therefore the use of multiple thresholds is recommended.<sup>46</sup> So, taking a whole human mandible into account, as is clinically relevant in reconstructive, trauma, and orthognathic surgery, segmentation procedures would probably be more elaborate and may result in more geometric inaccuracies than reported in this study. This is particularly relevant in CBCT imaging due to the constraints outlined above. Therefore, the accuracy reported in this study is not fully applicable to clinical conditions.

## 5 | CONCLUSIONS

In conclusion, 3-dimensional T1-weighted MRI was as well suited as CT and CBCT for providing accurate virtual 3-dimensional bone surface models of the mandible. These findings have a substantial clinical impact because MRI avoids any exposure to radiation for the patient and has some additional diagnostic benefits due to its excellent soft tissue contrast. Further studies are necessary to compare different imaging protocols as well as different segmentation techniques and to transfer the MRI-based approach to clinical settings.

## ACKNOWLEDGMENTS

The authors did not receive financial or material support. MRI examinations were covered by in-house funds of the Department of Diagnostic and Interventional Neuroradiology, Klinikum Rechts der Isar, Technische Universität München, Germany. This manuscript includes results of a current doctoral thesis work of Plamena Lyutskanova at Faculty of Medicine, Ludwig-Maximilians-Universität München.

Open access funding enabled and organized by Projekt DEAL.

## CONFLICT OF INTEREST

Florian Andreas Probst, Maria Juliane Stumbaum, and Monika Probst have applied for a German patent on the subject of a device and method to support imaging of MRI. Dimitrios Karampinos reports grants from Philips Healthcare outside the submitted work. The other authors declare no conflict of interest.

## AUTHOR CONTRIBUTIONS

Florian Andreas Probst and Monika Probst contributed to the study conception and design, data acquisition, data analysis and interpretation, and the writing and revision of the manuscript. Yoana Malenova and Plamena Lyutskanova contributed to data acquisition, data analysis and interpretation, and the revision of the manuscript. Maria

Juliane Stumbaum contributed to the study conception and design, data acquisition, and revision of the manuscript. Lucas Maximilian Ritsch contributed to data analysis and interpretation, and the revision of the manuscript. Dimitrios Karampinos and Sophia Kronthaler contributed to data acquisition, data analysis, and the revision of the manuscript. Egon Burian contributed to data acquisition, data analysis and interpretation, and the revision of the manuscript. All authors reviewed and approved the final version of the manuscript and agreed to be accountable for all aspects of work ensuring integrity and accuracy.

#### DATA AVAILABILITY STATEMENT

The data that support the findings of this study are available from the corresponding author upon reasonable request.

#### ORCID

Florian Andreas Probst  <https://orcid.org/0000-0002-0261-2030>

#### REFERENCES

- Elnagar MH, Aronovich S, Kusnoto B. Digital workflow for combined orthodontics and orthognathic surgery. *Oral Maxillofac Surg Clin North Am.* 2020;32(1):1-14.
- Deeb GR, Tran DQ, Deeb JG. Computer-aided planning and placement in implant surgery. *Atlas Oral Maxillofac Surg Clin North Am.* 2020;28(2):53-58.
- Tahmaseb A, Wu V, Wismeijer D, Coucke W, Evans C. The accuracy of static computer-aided implant surgery: a systematic review and meta-analysis. *Clin Oral Implants Res.* 2018;29(Suppl 16):416-435.
- Amundson M, Newman M, Cheng A, Khatib B, Cuddy K, Patel A. Three-dimensional computer-assisted surgical planning, manufacturing, intraoperative navigation, and computed tomography in maxillofacial trauma. *Atlas Oral Maxillofac Surg Clin North Am.* 2020;28(2):119-127.
- van Baar GJC, Forouzanfar T, Liberton N, Winters HAH, Leusink FKJ. Accuracy of computer-assisted surgery in mandibular reconstruction: a systematic review. *Oral Oncol.* 2018;84:52-60.
- Laure B, Louisy A, Joly A, Travers N, Listrat A, Pare A. Virtual 3D planning of osteotomies for craniosynostoses and complex craniofacial malformations. *Neurochirurgie.* 2019;65(5):269-278.
- Sakai Y, Okamura K, Kitamoto E, et al. Improved scan method for dental imaging using multidetector computed tomography: a phantom study. *Dentomaxillofac Radiol.* 2020;49(6):20190462.
- Yeung AWK, Jacobs R, Bornstein MM. Novel low-dose protocols using cone beam computed tomography in dental medicine: a review focusing on indications, limitations, and future possibilities. *Clin Oral Investig.* 2019;23(6):2573-2581.
- Han MA, Kim JH. Diagnostic X-ray exposure and thyroid cancer risk: systematic review and meta-analysis. *Thyroid.* 2018;28(2):220-228.
- Memon A, Rogers I, Paudyal P, Sundin J. Dental X-rays and the risk of thyroid cancer and meningioma: a systematic review and meta-analysis of current epidemiological evidence. *Thyroid.* 2019;29(11):1572-1593.
- Mastrogiacomo S, Dou W, Jansen JA, Walboomers XF. Magnetic resonance imaging of hard tissues and hard tissue engineered bio-substitutes. *Mol Imaging Biol.* 2019;21(6):1003-1019.
- Siriwanarangsun P, Statum S, Biswas R, Bae WC, Chung CB. Ultra-short time to echo magnetic resonance techniques for the musculo-skeletal system. *Quant Imaging Med Surg.* 2016;6(6):731-743.
- Sollmann N, Loffler MT, Kronthaler S, et al. MRI-based quantitative osteoporosis imaging at the spine and femur. *J Magn Reson Imaging.* 2020;54(1):12-35.
- Assaf AT, Zrnc TA, Remus CC, et al. Evaluation of four different optimized magnetic-resonance-imaging sequences for visualization of dental and maxillo-mandibular structures at 3 T. *J Craniomaxillofac Surg.* 2014;42(7):1356-1363.
- Flugge T, Hovener JB, Ludwig U, et al. Magnetic resonance imaging of intraoral hard and soft tissues using an intraoral coil and FLASH sequences. *Eur Radiol.* 2016;26(12):4616-4623.
- Hilgenfeld T, Prager M, Heil A, et al. PETRA, MSVAT-SPACE and SEMAC sequences for metal artefact reduction in dental MR imaging. *Eur Radiol.* 2017;27(12):5104-5112.
- Ludwig U, Eisenbeiss AK, Scheifele C, et al. Dental MRI using wireless intraoral coils. *Sci Rep.* 2016;6:23301.
- Prager M, Heiland S, Gareis D, Hilgenfeld T, Bendszus M, Gaudio C. Dental MRI using a dedicated RF-coil at 3 Tesla. *J Craniomaxillofac Surg.* 2015;43(10):2175-2182.
- Duttenhoefer F, Mertens ME, Vizkelely J, Gremse F, Stadelmann VA, Sauerbier S. Magnetic resonance imaging in zirconia-based dental implantology. *Clin Oral Implants Res.* 2015;26(10):1195-1202.
- Goto TK, Nishida S, Nakamura Y, et al. The accuracy of 3-dimensional magnetic resonance 3D vbe images of the mandible: an in vitro comparison of magnetic resonance imaging and computed tomography. *Oral Surg Oral Med Oral Pathol Oral Radiol Endod.* 2007;103(4):550-559.
- Juerchott A, Freudspurger C, Weber D, et al. In vivo comparison of MRI- and CBCT-based 3D cephalometric analysis: beginning of a non-ionizing diagnostic era in craniomaxillofacial imaging? *Eur Radiol.* 2020;30(3):1488-1497.
- van Eijnatten M, Rijkhorst EJ, Hofman M, Forouzanfar T, Wolff J. The accuracy of ultrashort echo time MRI sequences for medical additive manufacturing. *Dentomaxillofac Radiol.* 2016;45(5):20150424.
- Lee YS, Seon JK, Shin VI, Kim GH, Jeon M. Anatomical evaluation of CT-MRI combined femoral model. *Biomed Eng Online.* 2008;7:6.
- Neubert A, Wilson KJ, Engstrom C, et al. Comparison of 3D bone models of the knee joint derived from CT and 3T MR imaging. *Eur J Radiol.* 2017;93:178-184.
- Rathnayaka K, Momot KI, Noser H, et al. Quantification of the accuracy of MRI generated 3D models of long bones compared to CT generated 3D models. *Med Eng Phys.* 2012;34(3):357-363.
- Stephen JM, Calder JD, Williams A, El Daou H. Comparative accuracy of lower limb bone geometry determined using MRI, CT and direct bone 3D models. *J Orthop Res.* 2020. <https://doi.org/10.1002/jor.24923>. Online ahead of print.
- Van den Broeck J, Vereecke E, Wirix-Speetjens R, Vander SJ. Segmentation accuracy of long bones. *Med Eng Phys.* 2014;36(7):949-953.
- Agbaje JO, de Castele EV, Salem AS, Anumendem D, Lambrechts I, Politis C. Tracking of the inferior alveolar nerve: its implication in surgical planning. *Clin Oral Investig.* 2017;21(7):2213-2220.
- Burian E, Probst FA, Weidlich D, et al. MRI of the inferior alveolar nerve and lingual nerve-anatomical variation and morphometric benchmark values of nerve diameters in healthy subjects. *Clin Oral Investig.* 2019;24(8):2625-2634.
- Burian E, Sollmann N, Ritschl LM, et al. High resolution MRI for quantitative assessment of inferior alveolar nerve impairment in course of mandible fractures: an imaging feasibility study. *Sci Rep.* 2020;10(1):11566.
- Hilgenfeld T, Kastel T, Heil A, et al. High-resolution dental magnetic resonance imaging for planning palatal graft surgery—a clinical pilot study. *J Clin Periodontol.* 2018;45(4):462-470.
- Probst FA, Schweiger J, Stumbaum MJ, Karampinos D, Burian E, Probst M. Magnetic resonance imaging based computer-guided dental implant surgery—a clinical pilot study. *Clin Implant Dent Relat Res.* 2020;22(5):612-621.

33. Probst M, Richter V, Weitz J, et al. Magnetic resonance imaging of the inferior alveolar nerve with special regard to metal artifact reduction. *J Craniomaxillofac Surg*. 2017;45(4):558-569.
34. Gersing AS, Pfeiffer D, Kopp FK, et al. Evaluation of MR-derived CT-like images and simulated radiographs compared to conventional radiography in patients with benign and malignant bone tumors. *Eur Radiol*. 2019;29(1):13-21.
35. van Eijnatten M, van Dijk R, Dobbe J, Streekstra G, Koivisto J, Wolff J. CT image segmentation methods for bone used in medical additive manufacturing. *Med Eng Phys*. 2018;51:6-16.
36. Gelaude F, Vander Sloten J, Lauwers B. Accuracy assessment of CT-based outer surface femur meshes. *Comput Aided Surg*. 2008;13(4):188-199.
37. Huotilainen E, Paloheimo M, Salmi M, et al. Imaging requirements for medical applications of additive manufacturing. *Acta Radiol*. 2014;55(1):78-85.
38. Martelli N, Serrano C, van den Brink H, et al. Advantages and disadvantages of 3-dimensional printing in surgery: a systematic review. *Surgery*. 2016;159(6):1485-1500.
39. Smith EJ, Anstey JA, Venne G, Ellis RE. Using additive manufacturing in accuracy evaluation of reconstructions from computed tomography. *Proc Inst Mech Eng H*. 2013;227(5):551-559.
40. Huotilainen E, Jaanimets R, Valasek J, et al. Inaccuracies in additive manufactured medical skull models caused by the DICOM to STL conversion process. *J Craniomaxillofac Surg*. 2014;42(5):e259-e265.
41. Fourie Z, Damstra J, Schepers RH, Gerrits PO, Ren Y. Segmentation process significantly influences the accuracy of 3D surface models derived from cone beam computed tomography. *Eur J Radiol*. 2012;81(4):e524-e530.
42. Geiger D, Bae WC, Statum S, Du J, Chung CB. Quantitative 3D ultrashort time-to-echo (UTE) MRI and micro-CT (muCT) evaluation of the temporomandibular joint (TMJ) condylar morphology. *Skeletal Radiol*. 2014;43(1):19-25.
43. Antila K, Lilja M, Kalke M. Segmentation of facial bone surfaces by patch growing from cone beam CT volumes. *Dentomaxillofac Radiol*. 2016;45(8):20150435.
44. Engelbrecht WP, Fourie Z, Damstra J, Gerrits PO, Ren Y. The influence of the segmentation process on 3D measurements from cone beam computed tomography-derived surface models. *Clin Oral Investig*. 2013;17(8):1919-1927.
45. Loubele M, Maes F, Schutyser F, Marchal G, Jacobs R, Suetens P. Assessment of bone segmentation quality of cone-beam CT versus multislice spiral CT: a pilot study. *Oral Surg Oral Med Oral Pathol Oral Radiol Endod*. 2006;102(2):225-234.
46. van Eijnatten M, Koivisto J, Karhu K, Forouzanfar T, Wolff J. The impact of manual threshold selection in medical additive manufacturing. *Int J Comput Assist Radiol Surg*. 2017;12(4):607-615.
47. Gersing AS, Bodden J, Neumann J, et al. Accelerating anatomical 2D turbo spin echo imaging of the ankle using compressed sensing. *Eur J Radiol*. 2019;118:277-284.
48. Monch S, Sollmann N, Hock A, Zimmer C, Kirschke JS, Hedderich DM. Magnetic resonance imaging of the brain using compressed sensing—quality assessment in daily clinical routine. *Clin Neuroradiol*. 2019;30(2):279-286.
49. Flugge T, Derksen W, Te Poel J, Hassan B, Nelson K, Wismeijer D. Registration of cone beam computed tomography data and intraoral surface scans—a prerequisite for guided implant surgery with CAD/CAM drilling guides. *Clin Oral Implants Res*. 2017;28(9):1113-1118.
50. Hilgenfeld T, Juerchott A, Deisenhofer UK, et al. In vivo accuracy of tooth surface reconstruction based on CBCT and dental MRI—a clinical pilot study. *Clin Oral Implants Res*. 2019;30(9):920-927.
51. Flugge T, Ludwig U, Hovener JB, Kohal R, Wismeijer D, Nelson K. Virtual implant planning and fully guided implant surgery using magnetic resonance imaging—proof of principle. *Clin Oral Implants Res*. 2020;31:575-583.
52. Hilgenfeld T, Juerchott A, Jende JME, et al. Use of dental MRI for radiation-free guided dental implant planning: a prospective, in vivo study of accuracy and reliability. *Eur Radiol*. 2020;30(12):6392-6401.
53. Lethaus B, Gruichev D, Grafe D, et al. “Black bone”: the new backbone in CAD/CAM-assisted craniocystostomy surgery? *Acta Neurochir*. 2020;163:1735-1741.
54. Eley KA, Delso G. Automated segmentation of the craniofacial skeleton with “black bone” magnetic resonance imaging. *J Craniofac Surg*. 2020;31(4):1015-1017.
55. Eley KA, Delso G. Automated 3D MRI rendering of the craniofacial skeleton: using ZTE to drive the segmentation of black bone and FIESTA-C images. *Neuroradiology*. 2020;63(1):91-98.

**How to cite this article:** Probst FA, Burian E, Malenova Y, et al. Geometric accuracy of magnetic resonance imaging-derived virtual 3-dimensional bone surface models of the mandible in comparison to computed tomography and cone beam computed tomography: A porcine cadaver study. *Clin Implant Dent Relat Res*. 2021;23(5):779-788. <https://doi.org/10.1111/cid.13033>